Journal of Alloys and Compounds 506 (2010) 63–69

Contents lists available at ScienceDirect

Journal of Alloys and Compounds

journal homepage: www.elsevier.com/locate/jallcom

Application of a new kinetic model for the hydriding kinetics of $LaNi_{5-x}Al_x$ ($0 \le x \le 1.0$) alloys

X.H. An, Y.B. Pan, Q. Luo, X. Zhang, J.Y. Zhang, Q. Li*

Shanghai Key Laboratory of Modern Metallurgy & Materials Processing, Shanghai University, Shanghai 200072, PR China

ARTICLE INFO

Article history:
Received 27 March 2010
Received in revised form 28 June 2010
Accepted 6 July 2010
Available online 14 July 2010

Keywords:
Hydrogen absorbing materials
Metal hydrides
Gas–solid reactions
Kinetics

ABSTRACT

The hydriding kinetic mechanism of $LaNi_{5-x}Al_x$ ($0 \le x \le 1.0$) is clarified using Chou model, involving the influence of temperature, pressure and Al content. The results indicate that the rate-controlling step of the hydriding reaction in $LaNi_5$ and $LaNi_{4.7}Al_{0.3}$ is diffusion, but in $LaNi_4Al$, it is surface penetration at the temperature range of 30–80 °C. Moreover, the hydriding reaction rates increase with increasing temperature for the three alloys. Based on the results calculated using the Chou model, the rate-controlling steps for $LaNi_5$ and $LaNi_{4.7}Al_{0.3}$ correspond to surface penetration and diffusion under different pressures ranging from 0.47 to 1.0 MPa, and the hydrogenation rate increases with an increase in pressure. A suitable addition of Al can obviously improve the hydrogen absorption reaction rate. For $LaNi_{5-x}Al_x$ ($x = 0$, 0.15, 0.5 and 1.0) under a hydrogen pressure of 1.00 MPa at 30 °C, the hydrogen absorption reaction rate is as follows: $LaNi_5 < LaNi_4Al < LaNi_{4.5}Al_{0.5} < LaNi_{4.85}Al_{0.15}$.

1. Introduction

$LaNi_5$-type hydrogen storage alloys hold an important position among hydride-forming alloys owing to its significant hydrogen storage capacity and favorable absorption/desorption characteristics [1]. At present, partial replacement of Ni in $LaNi_5$ by a third element is usually employed to improve hydriding properties for practical applications [2]. Some studies have focused on Al-substituted alloys from an engineering viewpoint because suitable addition of Al can reduce plateau pressure and enhance reaction kinetics [3].

The kinetics of $LaNi_{5-x}Al_x$ has been investigated by many researchers and much attention has been devoted to revealing their hydriding/dehydriding reaction kinetic mechanism [4–6]. Recent studies on the absorption kinetic mechanism for $LaNi_{5-x}Al_x$ have been conducted using classical models, such as the first order model [4], the shrinking core model [7], the nucleation and growth model [7], the Jander model [8] and the Johnson–Mehl–Avrami (JMA) model [8]. The kinetics of $LaNi_{5-x}Al_x$ has also been investigated using other models which are derived from different assumptions to illustrate the kinetic mechanism. Jae et al. [9] have deduced a model on the assumption that the $LaNi_{4.5}Al_{0.5}$ particles are homogeneous spheres with a uniform diameter and no density change in the particles after the hydriding reaction. Dhaou and Askri [10] have derived empirical rate equations based on the gas–solid reaction kinetics to study the hydrogen absorption reaction kinetic behavior of $LaNi_5$, $LaNi_{4.85}Al_{0.15}$ and $LaNi_{4.75}Fe_{0.25}$. Martin et al. [11] have assumed that one of physisorption, chemisorption, surface penetration, diffusion and hydride formation may be the rate-controlling step and deduced a series of equations to clarify the hydriding/dehydriding kinetic mechanism of $LaNi_{4.7}Al_{0.3}$. Although a number of kinetic models are well applied to elucidate the kinetic mechanism of $LaNi_{5-x}Al_x$, there has not been a consistent conclusion about the rate-controlling step for the hydrogenation reaction of $LaNi_{5-x}Al_x$.

In this paper, the experimental data of $LaNi_{5-x}Al_x$ ($x = 0$, 0.15 and 0.3) have been summarized from literatures [8,10,11]. The absorption kinetics of $LaNi_{4.5}Al_{0.5}$ and $LaNi_4Al$ was measured in order to systematically study the effect of Al content on the absorption reaction kinetics of $LaNi_5$. The influence of temperature, pressure and Al content on the kinetic mechanism of $LaNi_{5-x}Al_x$ was investigated through the Chou model [12,13] using a few programming steps on a personal computer. All the calculated results have been compared with the experimental data.

2. Experimental and kinetic model

2.1. Experimental

The $LaNi_{4.5}Al_{0.5}$ and $LaNi_4Al$ alloys were synthesized from pure components through induction melting under an argon atmosphere. The mass purity of lanthanum, nickel and aluminum was 99.83%, 99.99% and 99.99%, respectively. The final compositions of the samples were confirmed using chemical analysis. X-ray power

* Corresponding author. Tel.: +86 21 56334045; fax: +86 21 56338065.
E-mail addresses: shuliqian@shu.edu.cn, qian246@hotmail.com (Q. Li).

0925-8388/$ – see front matter © 2010 Elsevier B.V. All rights reserved.
doi:10.1016/j.jallcom.2010.07.016

Table 1
Kinetic expressions describing the hydriding reaction in $LaNi_{5-x}Al_x$.

No.	Kinetic model	Comments	Reference
1	$\xi = 1-(1-Kt)^3$	Shrinking core model	[7]
2	$\xi = 1-\exp[-(Kt)^n]$	JMA model	[8]
3	$\xi = 1-(1-\sqrt{Kt})^3$	Jander model	[8]
4	$\xi = 1-n\exp-(Kt)$	Nucleation and growth model	[14]
5	$\xi = 1-\exp\left[-K(N-1)\frac{\ln(P_H/P_{eq})}{(P_H/P_{eq})}t\right]$	Analyzing absorption kinetics	[10]
6	$\xi = 1-\left[1-\sqrt{\frac{2D_H^0K_{sp}^0\sqrt{K_{ca}^0K_{pa}^0}(\sqrt{P_H}-\sqrt{P_{eq}})\exp(-((E_{\nu(d)})/RT))}{R_0^2\nu_m}t}\right]^3$	Diffusion is the rate limiting step	[12,13]
7	$\xi = 1-\left[1-\frac{K_{sp}^0\sqrt{K_{pa}^0K_{ca}^0}(\sqrt{P_H}-\sqrt{P_{eq}})\exp(-((E_{\nu(sp)})/RT))}{R_0\nu_m}t\right]^3$	Surface penetration is the rate limiting step	[12,13]

diffraction (XRD) measurements were performed on both samples before the hydriding kinetic measurement. The XRD measurements were carried out on a DLMAX-2200 diffractometer (CuKα radiation, $10^\circ \le 2\theta \le 90^\circ$) operated at 40 kV and 200 mA. The Materials Data Inc. software Jade 5.0 and a Powder Diffraction File were used to analyze the XRD data of both samples. The samples were firstly activated through absorption/desorption cycles and then the absorption kinetic measurement was performed at 30 and 40 °C under 1.00 MPa. The absorption kinetics was measured using a volumetric method with high purity hydrogen (99.999%).

2.2. Kinetic model

The model fitting method is extensively used to investigate the hydriding/dehydriding reaction kinetics of AB_5-type hydrogen storage alloys in a gas–solid reaction. A number of investigators have studied the kinetic mechanisms of $LaNi_{5-x}Al_x$ using different models. Their results are partly summarized and listed in Table 1. Haberman et al. [7] have reported that both the shrinking core model and the nucleation and growth model were applicable to the absorption reaction mechanism of $LaNi_{4.75}Al_{0.25}$, and the activation energy was equal to 24.1 kJ/mol. Zhang et al. [4] have concluded that the addition of Al reduced the absorption and desorption reaction rates of $LaNi_{5-x}Al_x$ ($0 \le x \le 0.3$) at 40 °C based on the first order model and that the rate-controlling step changed from the chemisorption of hydrogen on the surface to the conversion of α-phase to β-phase during hydrogen absorption. Muthukumar et al. [8] have employed the Jander and JMA models simultaneously to study the hydriding reaction kinetics of $LaNi_5$ and $LaNi_{4.7}Al_{0.3}$. They have claimed that the rate-controlling mechanism in the (α + β)-phase region is the diffusion of the hydride atom into the metal hydride, and they found that the activation energy for $LaNi_{4.7}Al_{0.3}$ was larger than that of $LaNi_5$. Jae et al. [9] have supposed that the dissociative chemisorption of the hydrogen molecule on the surface was the rate-controlling step for the hydriding reaction of $LaNi_{4.5}Al_{0.5}$, which had an activation energy of 39.73 kJ/mol. Dhaou and Askri [10] have assumed that both Fe and Al could improve the hydriding kinetics of $LaNi_5$ in the temperature range of 0–80 °C and that the chemical reaction was the rate-controlling step. Martin et al. [11] have considered chemisorption as the slowest step in the hydrogen absorption reaction of $LaNi_{4.7}Al_{0.3}$. Wang and Suda [15] have derived a rate equation by taking account of the reversible nature of the hydriding reaction in $LaNi_{4.7}Al_{0.3}$–H system. They have reported that the reaction rates in the α and β-phases were much faster than those in the two-phase (α + β) region.

Numerous kinetic functions on the absorption kinetics of $LaNi_{5-x}Al_x$ are available in literatures. However, different researchers obtained different results and conclusions. Furthermore, it is difficult for these models to offer an explicit analytic expression and provide an intuitive quantitative discussion. Therefore, we select the Chou model in this work because it offers an explicit analytic expression including parameters with clear physical representation. For example, the characteristic reaction time (t_c) in the Chou model can be directly used to identify the reaction rate quantitatively.

For surface penetration, the essential limiting rate can be expressed as Eq. (7) in Table 1. Here, we can define:

$$t_{c(sp)} = \frac{R_0\nu_m}{K_{sp}^0\sqrt{K_{pa}^0K_{ca}^0}(\sqrt{P_H}-\sqrt{P_{eq}})\exp(-((E_{\nu(sp)})/RT))} \quad (1)$$

Combining Eq. (1) and Eq. (7) in Table 1, we obtain:

$$\xi = 1-\left(1-\frac{t}{t_{c(sp)}}\right)^3 \quad (2)$$

where $t_{c(sp)}$ is the characteristic time when the rate-controlling step is surface penetration. When $t = t_{c(sp)}$, $\xi = 1$. Therefore, the physical meaning of the characteristic reaction time is the time required for the reaction to be completed. A smaller t_c value represents a faster reaction process. When the rate-controlling step is diffusion, the relation between the fraction (ξ) and time (t) can be illustrated as Eq. (6). This is defined as:

$$t_{c(d)} = \frac{R_0^2\nu_m}{2D_H^0K_{sp}^0\sqrt{K_{ca}^0K_{pa}^0}(\sqrt{P_H}-\sqrt{P_{eq}})\exp(-((E_{\nu(d)})/rt))} \quad (3)$$

Substituting Eq. (3) into Eq. (6) yields:

$$\xi = 1-\left(1-\sqrt{\frac{t}{t_{c(d)}}}\right)^3 \quad (4)$$

where $t_{c(d)}$ is the characteristic time when the rate-controlling step is diffusion. For simplicity, Eqs. (2) and (4) are defined as surface penetration model and diffusion model, respectively, in the present work.

where ξ is the absorbed fraction at any time, K, K_{pa}^0, K_{ca}^0, K_{sp}^0, D, n are constant. t is the reacted time, t_c is the characteristic time. T (K) is the reaction temperature, $E_{\nu(sp)}$ and $E_{\nu(d)}$ (J/mol) are the activation energy of the reaction when the rate-controlling step is surface penetration and diffusion, respectively. R_0 is the radius of the particle, P_H (MPa) is partial pressure of hydrogen in gas phase, P_{eq} (MPa) is the hydrogen partial pressure in equilibrium with hydride, D_H^0 is a constant related to diffusion coefficient of hydrogen, and ν_m is coefficient depending on substance and reaction.

The error analysis is used to compare the theoretical data with the experimental data.

$$\Delta = \frac{1}{N}\cdot\sum\frac{\left|(\chi_i)_{mea}-(\chi_i)_{cal}\right|}{\left|(\chi_i)_{mea}\right|}\times 100\% \quad (5)$$

where Δ is an average relative error, $(\chi_i)_{mea}$ is experimental data, $(\chi_i)_{cal}$ is the value calculated from the model, and N is the sum of experimental points.

Table 2
The values of r^2, Δ (%) and t_c (s) of hydrogen absorption in $LaNi_{5-x}Al_x$ (x = 0, 0.3 and 1.0) with different models at different temperatures.

T (°C)	$LaNi_5$						$LaNi_{4.7}Al_{0.3}$						$LaNi_4Al$					
	Diffusion			Surface penetration			Diffusion			Surface penetration			Diffusion			Surface penetration		
	t_c (s)	r^2	Δ (%)	t_c (s)	r^2	Δ (%)	t_c (s)	r^2	Δ (%)	t_c (s)	r^2	Δ (%)	t_c (s)	r^2	Δ (%)	t_c (s)	r^2	Δ (%)
30	843.08	0.97	11.89	278.06	0.94	12.82	–	–	–	–	–	–	269.96	0.85	6.91	96.50	0.96	5.65
40	534.19		6.08	168.26		6.94	–	–	–	–	–	–	131.00		8.69	48.61		4.90
60	–	–	–	–	–	–	87.79	0.98	3.02	37.02	0.83	25.41	–	–	–	–	–	–
80	–	–	–	–	–	–	27.40		5.68	11.89		25.29	–	–	–	–	–	–

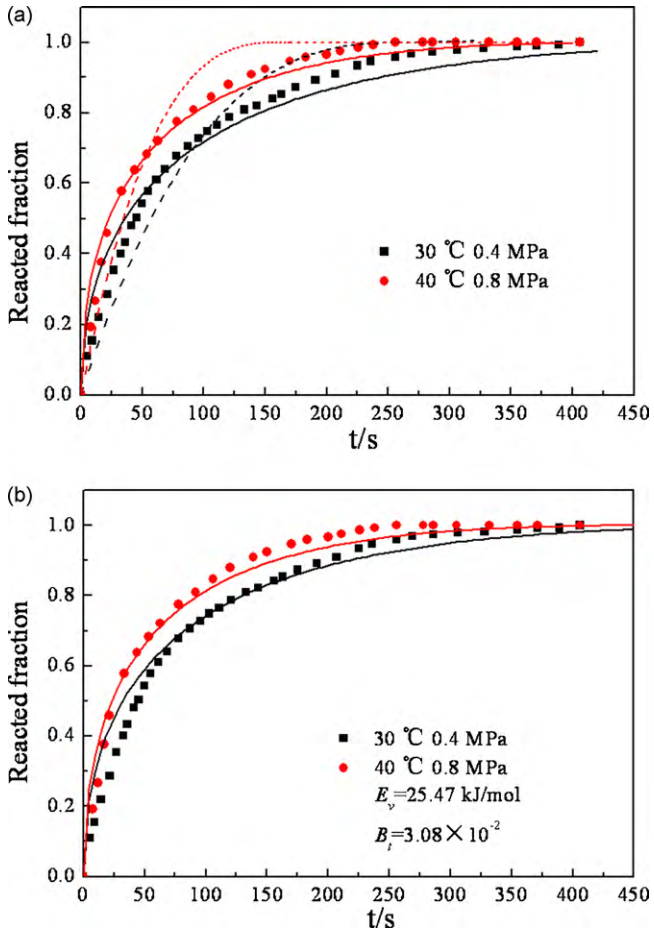

Fig. 1. Results of volumetric experiment on hydrogen absorption of $LaNi_{4.7}Al_{0.3}$ at different temperatures together with calculated curves (a) calculated with Eqs. (2) and (4) (solid: diffusion model, dash dot: surface penetration model) and (b) calculated with Eq. (6).

3. Results and discussion

3.1. *Effect of temperature on the absorption kinetics of $LaNi_5$, $LaNi_{4.7}Al_{0.3}$ and $LaNi_4Al$*

Muthukumar et al. [8] used the Jander model and the JMA model to investigate the hydriding kinetics of $LaNi_5$ and $LaNi_{4.7}Al_{0.3}$. Their experiment was carried out at 30, 40, 60 and 80 °C by keeping the pressure ratio at 2. They considered diffusion of the hydrogen atom into the metal hydride as the rate-controlling mechanism of $LaNi_5$ and $LaNi_{4.7}Al_{0.3}$. In the present work, the hydriding kinetic measurement for $LaNi_4Al$ was carried out at 30 and 40 °C under 1.00 MPa H_2. Moreover, the Chou model is employed to analyze the experimental data of $LaNi_5$, $LaNi_{4.7}Al_{0.3}$ and $LaNi_4Al$.

To determine the mechanism of the hydrogenation, the experimental data are processed using Eqs. (2) and (4). The calculated results, including r^2, Δ (%) and t_c (s), are shown in Table 2. For $LaNi_5$, Table 2 shows that the r^2 of the linear regression equations of the diffusion model is 0.97, while that of the surface penetration model is 0.94. Moreover, the calculated errors in the diffusion model are smaller than those in the surface penetration model. Fig. 1(a) presents the experimental data and calculated results, which illustrates that the fitting lines calculated from the diffusion model show a better agreement with the experimental data than the surface penetration model. Based on these results, we believe that diffusion is the rate-controlling step. Table 2 also shows that the characteristic time is 843.08 and 534.19 s at 30 and 40 °C, respec-

Table 3
The values of r^2, Δ (%) and t_c (s) of hydriding in $LaNi_{5-x}Al_x$ (x = 0 and 0.3) with different models under different pressure.

P (MPa)	$LaNi_5$						$LaNi_{4.7}Al_{0.3}$					
	Diffusion			Surface penetration			Diffusion			Surface penetration		
	t_c (s)	r^2	Δ (%)	t_c (s)	r^2	Δ (%)	t_c (s)	r^2	Δ (%)	t_c (s)	r^2	Δ (%)
0.47	–	–	–	–	–	–	35.80	0.98	4.31	11.26	0.92	12.44
0.62	–	–	–	–	–	–	32.07		5.43	8.43		16.50
0.78	–	–	–	–	–	–	25.87		8.95	6.35		8.96
0.60	829.13	0.90	16.25	272.04	0.99	2.83	–	–	–	–	–	–
0.80	705.79		12.71	250.27		4.28	–	–	–	–	–	–
1.00	678.70		7.78	239.66		5.60	–	–	–	–	–	–

tively, which indicates that the hydriding reaction rate increases with an increment in temperature.

The partial pressure of hydrogen in the gas phase is assumed to be fixed during the whole experimental process. When the rate-controlling step is diffusion, we can define B_t as a coefficient expressed by $B_t = R_0^2 \nu_m / 2D_H^0 K_{sp}^0 \sqrt{K_{ca}^0 K_{pa}^0}(\sqrt{P_H} - \sqrt{P_{eq}})$. Combining B_t, Eqs. (3) and (4) yields:

$$\xi = 1 - \left[1 - \exp\left(\frac{-E_{\nu(d)}}{2RT_\nu}\right) \cdot \sqrt{\frac{t}{B_t}}\right]^3 \quad (6)$$

When the surface penetration is the rate-controlling step, B_t can be defined as $B_t = R_0 \nu_m / K_{sp}^0 \sqrt{K_{pa}^0 K_{ca}^0}(\sqrt{P_H} - \sqrt{P_{eq}})$. Combining B_t, Eqs. (1) and (2) yields:

$$\xi = 1 - \left[1 - \exp\left(\frac{-E_{\nu(sp)}}{RT_\nu}\right) \cdot \frac{t}{B_t}\right]^3 \quad (7)$$

Eqs. (6) or (7) is used to calculate the activation energy when diffusion or surface penetration is the rate-controlling step. For $LaNi_5$, the rate-controlling step is treated as diffusion. Thus, Eq. (6) is employed to calculate the activation energy (25.47 kJ/mol) and coefficient (3.08×10^{-2}). The calculated curves are shown in Fig. 1(b), from which it can be seen that the experimental data can be well described with Eq. (6).

The same method is used to analyze the experimental data of $LaNi_{4.7}Al_{0.3}$ and $LaNi_4Al$. The calculated curves are shown in Figs. 2 and 3. Figs 2(a) and 3(a) show the calculated results using Eqs. (2) and (4). Figs. 2(b) and 3(b) present the results calculated from Eqs. (6) and (7), respectively. The r^2, Δ (%) and t_c (s), calculated from both the diffusion and surface penetration models, are also listed in Table 2. The results indicate that the rate-controlling step for the hydrogen absorption reaction in $LaNi_{4.7}Al_{0.3}$ is diffusion at 60 and 80 °C. In addition, the characteristic time reduces from 87.79 s at 60 °C to 27.40 s at 80 °C, which suggests that the hydriding reaction rate increases with an increase in temperature. The activation energy is calculated to be 48.23 kJ/mol and $B_t = 2.22 \times 10^{-6}$. For $LaNi_4Al$, surface penetration is the rate-controlling step, which can be obtained in view of Fig. 3(a) and Table 2. The characteristic time reduces from 96.50 to 48.61 s. The activation energy and B_t are calculated to be 44.06 kJ/mol and 2.42×10^{-6}, respectively.

Based on the results, we can conclude that the hydriding reaction rates increase with an increase in temperature for $LaNi_5$, $LaNi_{4.7}Al_{0.3}$ and $LaNi_4Al$. However, the rate-controlling step changes for different alloys, which may be attributed to the different experimental conditions.

3.2. Effect of pressure on the hydriding kinetics of $LaNi_5$ and $LaNi_{4.7}Al_{0.3}$

The experimental data of $LaNi_5$ and $LaNi_{4.7}Al_{0.3}$ are summarized from the references [10,11]. Dhaou and Askri [10] measured and analyzed the absorption kinetics of $LaNi_5$ at 30 °C and under the pressure range of 0.60–1.00 MPa. The absorption reaction kinetics data of $LaNi_{4.7}Al_{0.3}$ was also measured at 60 °C under different pressures (0.47, 0.62 and 0.78 MPa) by Martin et al. [11]. The hydrogenation kinetic behavior is shown in Figs. 4 and 5, which show plots of the hydrogen amount vs. time. Next, it is necessary to elucidate the relation between the hydrogenation amount and the reacted fraction, which can be expressed by:

$$\xi = \frac{\Delta m}{\Delta m_{max}} = \frac{(\Delta m / m_0)}{(\Delta m_{max} / m_0)} \quad (8)$$

where m is the reacted amount, m_0 is the initial weight of the sample, m/m_0 is the percentage of the reacted amount, and m_{max} is the maximum reacted amount.

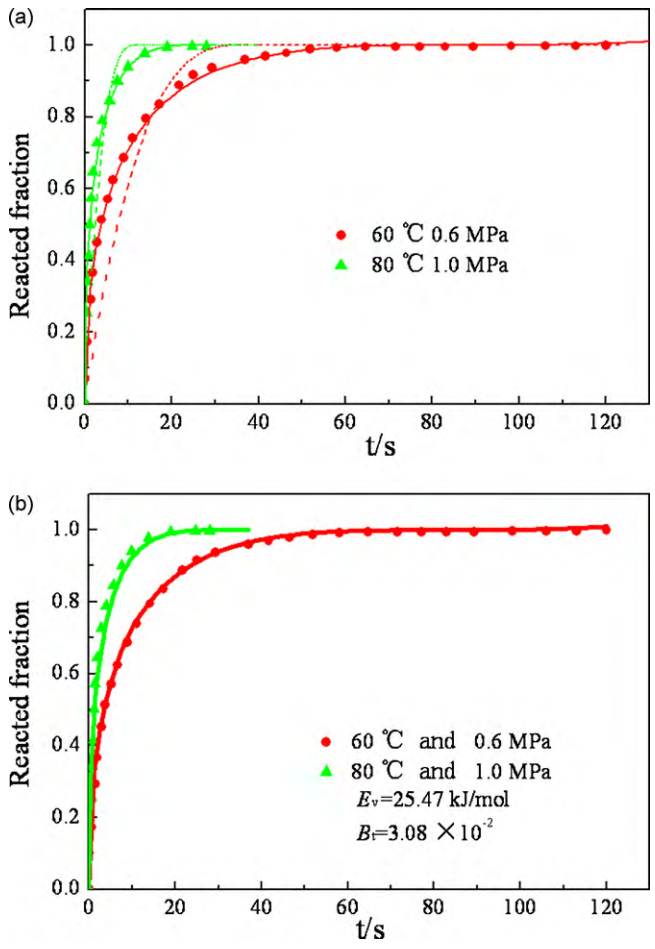

Fig. 2. Results of volumetric experiment on hydrogen absorption of $LaNi_5$ at different temperatures together with calculated curves (a) calculated with Eqs. (2) and (4) (solid: diffusion model, dash dot: surface penetration model) and (b) calculated with Eq. (6).

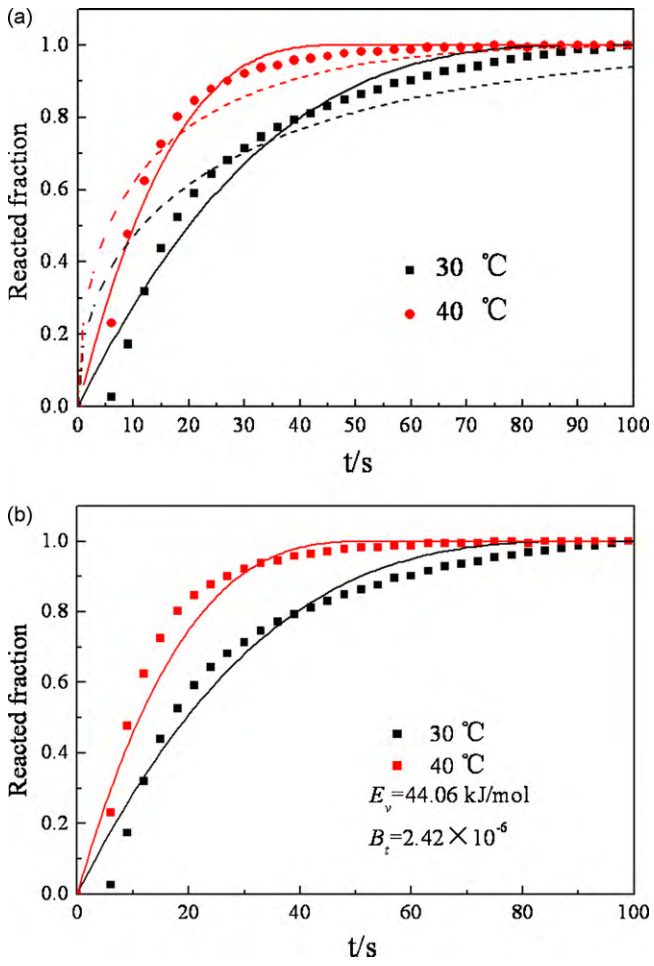

Fig. 3. Results of volumetric experiment on hydrogen absorption of $LaNi_4Al$ at 30 and 40 °C under 1.00 MPa H_2 together with calculated curves (a) calculated with Eqs. (2) and (4) (solid: surface penetration model, dash dot: diffusion model) and (b) calculated with Eq. (7).

Eqs. (2) and (4), together with Eq. (8), are used to interpret the experimental data of $LaNi_5$. The values of r^2, Δ (%) and t_c (s) are listed in Table 3. The r^2 for the diffusion model (0.90) is smaller than that for the surface penetration model (0.99). The error calculated by the diffusion model is larger than that of the surface penetration model. The calculated curves from surface penetration model display a better agreement with the experimental data than that from diffusion model (Fig. 4). Therefore, based on these results, surface penetration is the rate-controlling step. In addition, the characteristic times under 0.60, 0.80 and 1.00 MPa are calculated to be 272.04, 250.27 and 239.66 s, respectively, which indicates that the required time for $LaNi_5$ to completely hydride decreases with an increase in pressure. Namely, the hydrogenation reaction rate increases with an increase in pressure.

The experimental data of $LaNi_{4.7}Al_{0.3}$ is analyzed with the same method as mentioned above. The calculated results are also listed in Table 3. The r^2 for the diffusion model is 0.98, while that for the surface penetration model is only 0.92. Error calculated with the diffusion model is smaller than that with the surface penetration model. Fig. 5(a) presents the results calculated using Eqs. (2) and (4), which illustrate that the experimental data can be fitted with better accuracy by Eq. (4) than Eq. (2). Therefore, the rate-controlling step should be the diffusion of hydrogen atoms through the hydride product layer to the hydride/metal interface for this system from 0.47 to 0.78 MPa. The characteristic times under 0.47, 0.62 and 0.78 MPa are calculated to be 35.80, 32.07 and 25.87 s, respectively, which show that the required time for the $LaNi_{4.7}Al_{0.3}$ alloy to completely hydride gradually decreases as the initial pressure increased. Alternatively, the hydrogenation rate increases with an increase in initial pressure.

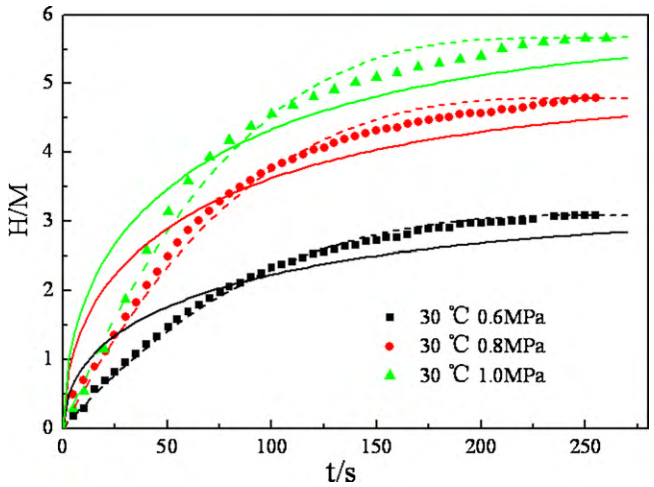

Fig. 4. Kinetic data of $LaNi_{4.7}Al_{0.3}$ alloys under different initial pressures at 70 °C together with calculated hydrogen absorption curves (solid: diffusion model, dash dot: surface penetration model).

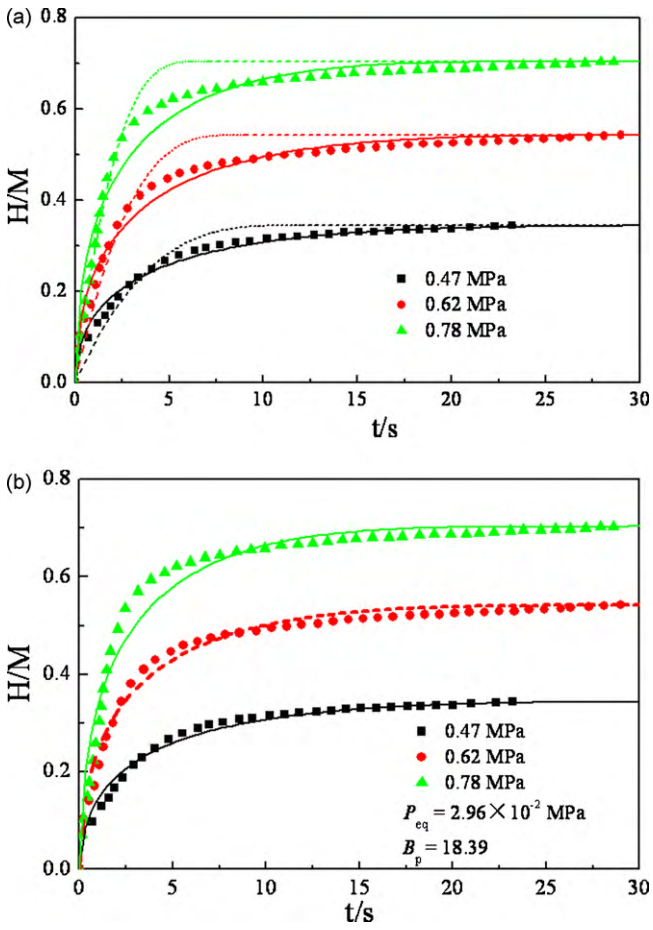

Fig. 5. Results of volumetric experiment on hydrogen absorption of $LaNi_5$ at different temperatures together with calculated curves (a) calculated with Eqs. (2) and (4) (solid: diffusion model, dash dot: surface penetration model) and (b) calculated and predicted curves with Chou model (solid: calculated with Eq. (9), dash dot: predicted with Eq. (10)).

The calculated results indicate that the rate-controlling step for the hydriding reaction in $LaNi_{4.7}Al_{0.3}$ is different from that in $LaNi_5$, which might be attributed to the different experimental conditions.

When the experiment is carried out at a constant temperature, we define another coefficient, B_p, as $B_p = R_0^2\nu_m/[2K_{sp}^0\sqrt{K_{pa}^0K_{ca}^0}D_H^0\exp(-E_{\nu(d)}/RT)]$. Combining B_p and Eqs. (3) and (4), the relationship of ξ and P_{eq} can be described as:

$$\xi = 1 - \left[1 - \sqrt{\frac{(\sqrt{P_H} - \sqrt{P_{eq}})\cdot t}{B_p}}\right]^3 \quad (9)$$

The Chou model can be used to not only calculate but also predict kinetic behavior at a specific pressure. Fig. 5(b) presents an example, which shows both the calculated and predicted curves using the Chou model. Eq. (9) is used to calculate the experimental data at 0.47 and 0.78 MPa, which are shown as solid curves in Fig. 5(b). The specific value of P_{eq} and B_p are found to be 2.96×10^{-2} MPa and 18.39, respectively. By substituting these two values into Eq. (9), Eq. (10) can be obtained. Using Eq. (10), the absorption kinetics of $LaNi_{4.7}Al_{0.3}$ at 0.62 MPa is predicted, as denoted by the dash dotted curve in Fig. 5(b), which suggests that both the calculated and predicted curves agree well with the experimental data.

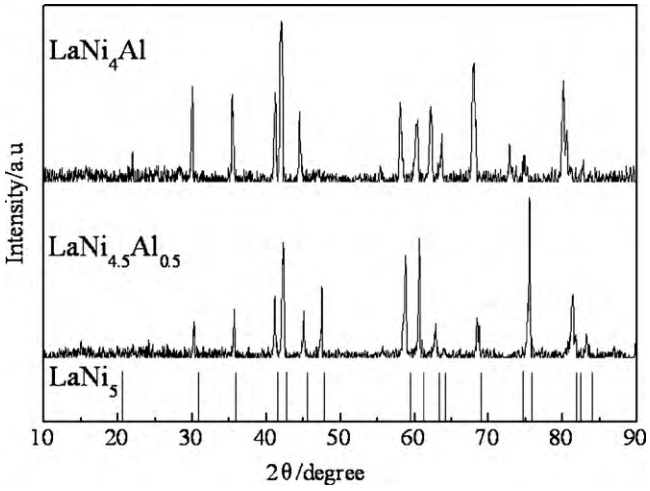

Fig. 6. XRD patterns for $LaNi_5$, $LaNi_{4.5}Al_{0.5}$ and $LaNi_4Al$.

$$\xi = 0.54 \times \left\{1 - \left[1 - \sqrt{\frac{(\sqrt{0.62} - \sqrt{2.96\times10^{-2}})\cdot t}{10.39}}\right]^3\right\} \quad (10)$$

3.3. Effect of Al amount substituting Ni on the hydriding kinetics rate of $LaNi_{5-x}Al_x$

Fig. 6 shows XRD patterns of the $LaNi_{4.5}Al_{0.5}$ and $LaNi_4Al$ alloys and the XRD pattern of $LaNi_5$ (PDF No. 17-0126). It can be seen that XRD patterns of the investigated alloys have homogeneous single phase corresponding to $CaCu_5$ type hexagonal structure with *P*6/*mmm* space group. The addition of Al causes the XRD peak to move left, which indicates that the cell volume of $LaNi_{4.5}Al_{0.5}$ and $LaNi_4Al$ alloys increases with increasing Al content, since the atomic radius of Al (1.43 å) is larger than that of Ni (1.24 å). The lattice gap becomes bigger as the cell volume increases, which may lead to an increase in the absorption reaction rate.

Dhaou and Askri [10] measured and analyzed the absorption kinetics of $LaNi_5$ and $LaNi_{4.85}Al_{0.15}$ at 30 °C and 1.00 MPa. In our work, in order to systematically investigate the effect of Al content on the absorption reaction kinetics of $LaNi_5$, we measured the kinetic behaviors of $LaNi_{4.5}Al_{0.5}$ and $LaNi_4Al$ according to the experimental conditions cited in Ref. [10]. The hydrogen absorption kinetics of $LaNi_{5-x}Al_x$ (x = 0, 0.15, 0.5 and 1.0) at 30 °C and 1.00 MPa is given in Fig. 7.

To determine which process is the slowest hydriding reaction step, both the diffusion and surface penetration models [Eqs. (2) and (4)] are applied to calculate the experimental data using the least square methods. The r^2, Δ (%) and t_c (s) calculated using dif-

Table 4
The values of r^2, Δ (%) and t_c (s) of $LaNi_{5-x}Al_x$ (x = 0, 0.15, 0.5 and 1.0) at 30 °C under 1.00 MPa.

	t_c(s)				r^2	Δ (%)
	$LaNi_5$	$LaNi_{4.85}Al_{0.15}$	$LaNi_{4.5}Al_{0.5}$	$LaNi_4Al$		
Surface penetration	240.59	27.23	81.28	96.50	0.99	4.95
Diffusion	680.36	93.13	217.32	269.96	0.90	14.01

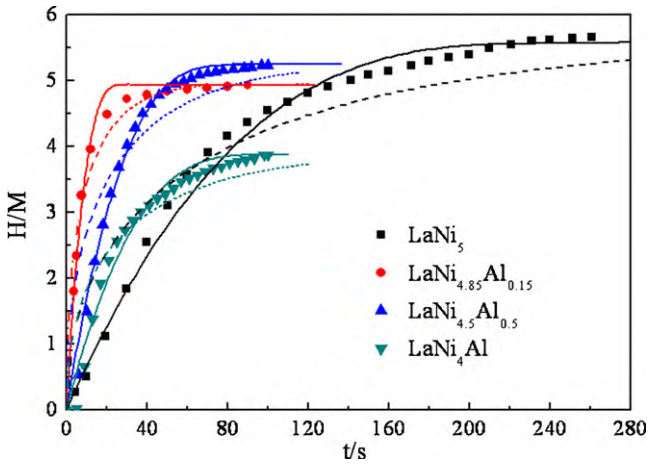

Fig. 7. Kinetic data of hydrogen absorption at 40 °C for $LaNi_{5-x}Al_x$ together with calculated curves (solid curves: surface penetration model, dash dot curves: diffusion model).

ferent models are listed in Table 4. The calculated curves are shown in Fig. 7, which indicate that the solid curves agree better with the experimental data than the dash dotted curves. This means that the rate-controlling step may be surface penetration.

According to Table 4, the corresponding r^2 of the linear regression equations is 0.99, and the average error is 4.95% for the surface penetration model. The r^2 and average error are 0.90 and 14.01% for the diffusion model, correspondingly, which indicates the rate–controlling step for absorption process is surface penetration. In addition, when x takes the value of 0, 0.15, 0.5 and 1.0, the characteristic times are 240.59, 27.23, 81.28 and 96.50 s, respectively. These calculated results suggest that the addition of Al increases the hydrogen absorption reaction rate which follows: $LaNi_5 < LaNi_4Al < LaNi_{4.5}Al_{0.5} < LaNi_{4.85}Al_{0.15}$. Based on these calculated results, the addition of Al increases the hydrogen absorption reaction rate, and there is an optimum value of Al addition for the amelioration of the kinetic property of $LaNi_5$. In other words, a suitable addition of Al can obviously improve the hydrogen absorption rate of $LaNi_{5-x}Al_x$ ($0 \le x \le 1.0$) alloys. Moreover, the rate-controlling step cannot be changed by increasing Al content at 30 °C and 1.00 MPa.

4. Conclusions

We used Chou model to investigate the hydriding mechanism of $LaNi_{5-x}Al_x$ ($0 \le x \le 1.0$) with focus on the influence of temperature, pressure and Al content. The results indicate that diffusion is the rate-controlling step for the hydriding reaction of $LaNi_5$ and $LaNi_{4.7}Al_{0.3}$, while surface penetration is the rate–controlling step for $LaNi_4Al$. The hydrogenation reaction rate increases with an increment in the operating temperatures from 30 to 80 °C. Under different pressures, the rate-controlling step for $LaNi_5$ is surface penetration, while, for $LaNi_{4.7}Al_{0.3}$, it is diffusion. The hydrogenation rate increases with an increase in pressure. For the hydrogen absorption process of $LaNi_{5-x}Al_x$ ($x = 0$, 0.15, 0.5 and 1.0), the corresponding r^2 of the linear regression equation is 0.99 and the error is 4.95% calculated with surface penetration model, and the order for the absorption reaction rate is as follows: $LaNi_5 < LaNi_4Al < LaNi_{4.5}Al_{0.5} < LaNi_{4.85}Al_{0.15}$.

Acknowledgements

The authors gratefully acknowledge the financial supports from the National Natural Science Foundation of China (50804029 and 50974084), a Foundation for the Author of National Excellent Doctoral Dissertation of PR China (200746), the Program for Changjiang Scholars and Innovative Research Team in University (IRT0739).

References

[1] M.H. Mendelsohn, D.M. Gruen, A.E. Dwight, J. Less-Common Met. 63 (1979) 193–207.
[2] S.L. Li, P. Wang, W. Chen, G. Luo, D.M. Chen, K. Yang, J. Alloys Compd. 485 (2009) 867–871.
[3] I.S. Park, J.K. Kim, K.J. Kim, J.X. Zhang, C. Park, K. Gawlik, Int. J. Hydrogen Energy 34 (2009) 5770–5777.
[4] W. Zhang, J. Cimato, A.J. Goudy, J. Alloys Compd. 201 (1993) 175–179.
[5] A.J. Goudy, R.A. Wallingford, J. Less-Common Met. 99 (1984) 249–256.
[6] X.L. Wang, S. Suda, J. Less-Common Met. 159 (1990) 83–90.
[7] Z. Haberman, J. Bloch, M.H. Mintz, J. Alloys Compd. 253–254 (1997) 556–559.
[8] P. Muthukumar, A. Satheesh, M. Linde, R. Mertz, M. Groll, Int. J. Hydrogen Energy 34 (2009) 7253–7262.
[9] W.O. Jae, Y.K. Chun, S.N. Kee, S.S. Kyu, J. Alloys Compd. 278 (1998) 270–276.
[10] H. Dhaou, F. Askri, Int. J. Hydrogen Energy 32 (2007) 576–587.
[11] M. Martin, C. Gommel, C. Borkhart, E. Fromm, J. Alloys Compd. 238 (1996) 193–201.
[12] K.C. Chou, K.D. Xu, Intermetallics 15 (2007) 767–777.
[13] K.C. Chou, J. Am. Ceram. Soc. 89 (2006) 1568–1576.
[14] J.W. Christian, The Theory of Transformations in Metals and Alloys, 3rd ed., Pergamon, Amsterdam, 2002.
[15] X.L. Wang, S. Suda, J. Less-Common Met. 159 (1990) 109–119.